Temperature Dependence of Current-Induced Magnetization Switching in Spin Valves with a Ferrimagnetic CoGd Free Layer

Xin Jiang,[1] Li Gao,[1,2] Jonathan Z. Sun,[3] and Stuart S. P. Parkin[1]
[1]*IBM Almaden Research Center, San Jose, California 95120, USA*
[2]*Department of Applied Physics, Stanford University, Stanford, California 94305, USA*
[3]*IBM T. J. Watson Research Center, Yorktown Heights, New York 10598, USA*
(Received 12 June 2006; published 20 November 2006)

The temperature dependence of current-induced magnetization switching of *ferrimagnetic* CoGd free layers in spin valves is explored. At temperatures well above and well below the magnetization compensation temperature (T_{MC}) of CoGd, a current flowing from the free layer to the CoFe fixed layer aligns the moments of the two layers parallel, and a current flowing in the opposite direction aligns them antiparallel. However, for intermediate temperatures just above T_{MC}, the current-induced alignment of the moments is reversed. We attribute this effect to the different compensation temperatures of the net magnetization and angular momentum of CoGd.

DOI: 10.1103/PhysRevLett.97.217202 PACS numbers: 75.75.+a, 72.25.−b, 75.60.Jk, 85.75.−d

When a spin-polarized current above a certain threshold passes through a magnetic nanostructure, the interaction between the conduction electron spins and the local angular momentum within the nanostructure becomes strong enough to cause magnetic excitations, leading to spin wave excitation and/or magnetization reversal [1–4]. This interaction can be viewed as a current-induced ''spin-transfer'' torque on the local magnetic moments. Spin-transfer torque provides a useful means of studying spin dynamics in nanoscale magnetic systems, and is also important technologically for applications ranging from magnetic sensors and memories to microwave-based communication technologies. To date, most research on current-induced magnetization switching (CIMS) has focused on spin valves or tunnel junctions with simple transition metal or alloy *ferromagnetic* layers [5]. An interesting magnetic system for CIMS studies is the family of ferrimagnetic rare-earth-transition-metal alloys, such as CoGd, for which the net magnetization can be continuously tuned across zero by varying its composition or temperature [6]. Moreover, the ferrimagnetic arrangement of the $3d$- and $4f$-shell magnetic moments in these alloys provides an intriguing test case for the verification of CIMS as an angular-momentum-driven process. Here we report the observation of CIMS in spin valves with a ferrimagnetic $Co_{74}Gd_{26}$ free layer. We demonstrate experimentally that the sign of the CIMS threshold current is associated with the net angular momentum, and not the net magnetic moment, of the antiferromagnetically aligned Co and Gd subnetworks in $Co_{74}Gd_{26}$.

Spin-valve devices were fabricated by using prepatterned stencil substrates [Fig. 1(a)], as described in detail elsewhere [7]. Briefly, stencils, comprised of nominally rectangularly shaped recesses with overhangs, were patterned in metal-insulator-metal multilayers using a combination of e-beam lithography, Ar ion milling, and wet etching. The size of the stencils varied from 50 nm by 50 nm up to 70 nm by 210 nm. Subsequently, multilayer thin films forming the stack of spin valves were deposited into the stencils at ambient temperature using magnetron sputtering. The film stack was comprised, from bottom to top, of 5 Pt|5 Ta|5 $Co_{74}Gd_{26}$|10 Cu|10 $Co_{70}Fe_{30}$|100 Cu, where the numbers indicate film thickness in nanometers. The CoFe and CoGd layers serve as the fixed and free layers, respectively. Optical lithography and Ar ion milling were used to define the top contact leads.

Transport measurements were conducted in a four-point contact geometry. An ac lock-in technique was used to measure the dynamic resistance $R_D = dV/dI$ of the spin valves in an in-plane magnetic field applied along the geometric easy axis (long axis of the rectangle), with an ac current excitation of 100 μA rms at 311 Hz. A dc bias current was simultaneously applied during the dV/dI measurements, with the positive direction corresponding to current flowing from the free to the fixed layer. The dynamic resistance was measured as a function of magnetic field and dc bias current at various temperatures. The inset of Fig. 1(b) shows a magnetoresistance (MR) loop at 290 K and zero bias current for a spin valve with a size of 50 nm by 200 nm. The external magnetic field aligns the moments of the CoFe and CoGd layers to be either parallel (P) or antiparallel (AP), resulting in an MR value of $\sim$0.5%, which is defined as $\mathrm{MR} = (R_{AP} - R_P)/R_P$, where R_{AP} (R_P) is the resistance of the AP (P) states. For the same device, a current sweep in zero magnetic field gives rise to a hysteretic change of R_D between a high and a low resistance state [Fig. 1(b)]. The resistance values of the two states are consistent with the R_{AP} and R_P values acquired in the magnetic field driven MR measurement, indicating that within experimental error ($\sim \pm 5\%$) a full magnetization reversal of the CoGd free layer is realized in the current sweep. The hysteretic CIMS is observed in fields below $\sim$250 Oe. In fields much larger than this, the variation of resistance with current becomes reversible

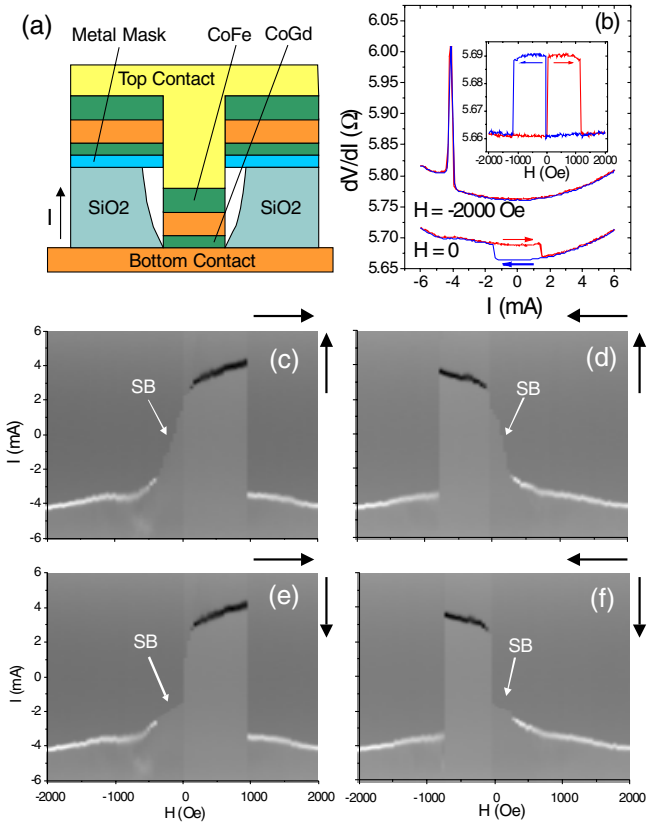

FIG. 1 (color online). (a) Schematic of a spin valve fabricated using a stencil substrate. (b) Dynamic resistance as a function of current measured in magnetic fields of 0 and −2000 Oe at 290 K. The inset shows the MR loop of the spin valve at 290 K. The arrows indicate the current and field sweep directions. (c)–(f) Contour plots of the dynamic resistance as a function of current and field. The data were acquired by sweeping current and stepping field. The arrows outside the contour plots indicate the directions in which the current and field are varied. The arrows inside the plots indicate the current-induced hysteretic switching boundaries (SB).

and a peak in dV/dI appears at a certain negative current value. Such a peak structure in $R_D(I)$ corresponds to a reversible step in the current-voltage characteristics.

More detailed dV/dI measurements were conducted by sweeping current in a constant field, and then repeating the sweep in a series of fields [Figs. 1(c)–1(f)]. The contrast in Figs. 1(c)–1(f) represents the resistance value of the spin valve. A lighter shade corresponds to a higher resistance value. Qualitatively, the results shown in Figs. 1(c)–1(f) are similar to those of Co/Cu/Co spin valves made with stencil substrates [7]. In the low field regime, current-induced hysteretic magnetization reversals are seen as switching boundaries between the dark and light regions in Figs. 1(c)–1(f). Resistance peaks in the high field regime are shown as white traces in the contour plots, whose positions vary linearly with field. Dark traces are seen in the intermediate field range, which may be related to reversible switching from the AP state to a lower resistance dynamic state [8]. Note that Figs. 1(c) and 1(e) are not exact mirror images of Figs. 1(d) and 1(f), which may indicate slight symmetry breaking due to, for instance, stray fields or pinning at the sample edges.

In the following, we focus on the temperature dependence of MR and zero-field CIMS. Figure 2(a) shows the $R_D(H)$ loops at various temperatures. MR is negative for temperatures below ~100 K: i.e., the resistance of the spin valve is larger when the CoFe and CoGd moments are aligned parallel by the field. Above ~150 K, the MR turns positive. Note that in the MR loops, a knee structure appears at low field, which we attribute to dipolar coupling between the spin-valve stack inside the stencil and the extended magnetic film above the stencil [7]. The extended magnetic film has small coercivity, hence switching at lower field. This introduces a small resistance change of ~10 mΩ. Figure 3 shows the temperature dependence of the switching fields for the CoFe layer, CoGd layer, and extended magnetic film. The temperature dependences are weak for the CoFe layer and the extended magnetic film. For the CoGd layer, however, the switching field shows a maximum at ~150 K, which is due to the decreased net magnetization of CoGd near the magnetization compensation point, and the presence of a finite intrinsic magnetic

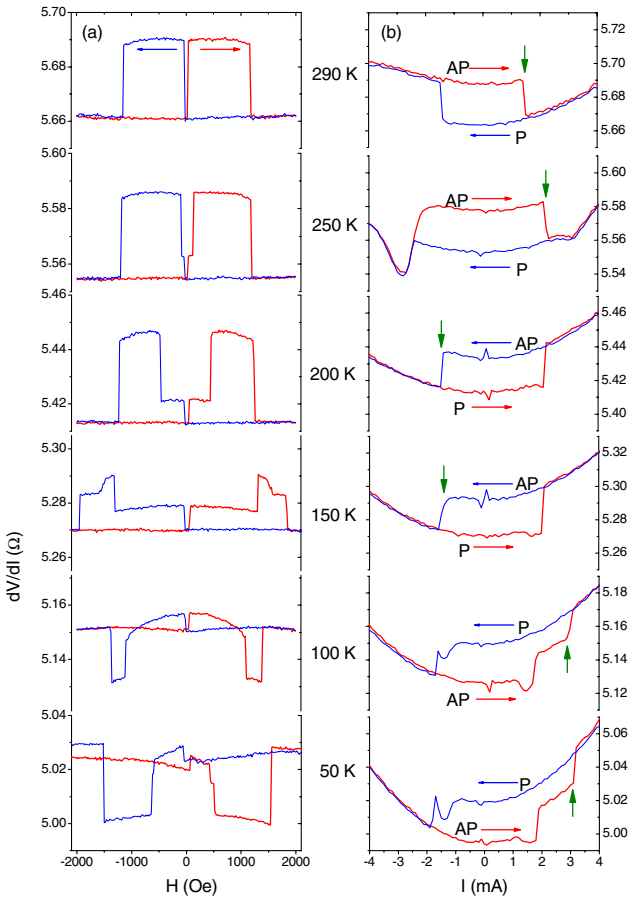

FIG. 2 (color online). MR (a) and zero-field CIMS (b) measured at various temperatures. P and AP in (b) indicate the relative alignment of the CoFe and CoGd magnetizations. The vertical arrows in (b) indicate CIMS from AP to P states.

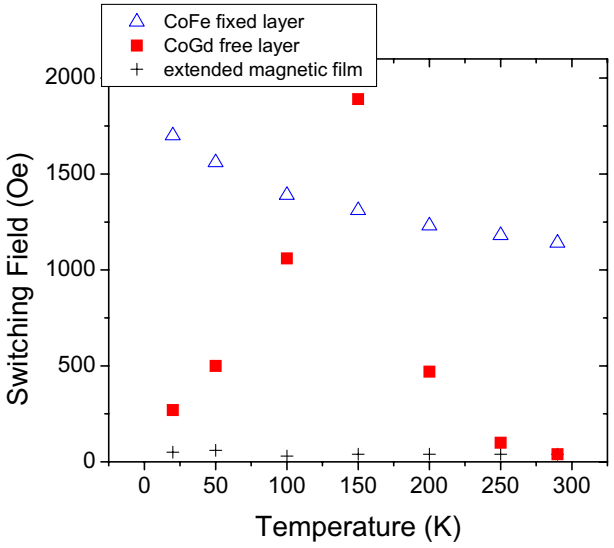

FIG. 3 (color online). Switching fields of the CoFe fixed layer, CoGd free layer, and extended magnetic film at different temperatures.

anisotropy that is only weakly temperature dependent across the compensation temperature region [9,10]. Note that the dipole field between the free and fixed layers affects the switching fields of both layers. The weak temperature dependence of the CoFe switching field suggests that the dipole field does not have a strong temperature dependence and thus cannot account for the observed diverging switching field of the free layer when its net magnetization approaches zero.

The temperature dependence of the CIMS thresholds are qualitatively different from that of the MR. For temperatures below ~100 K and above ~250 K, the characteristics of CIMS are the same as those observed in spin valves with transition metal ferromagnetic electrodes [5]: i.e., a positive current sweep switches the device from the AP to the P state; a negative current sweep switches the device from the P to the AP state. However, for intermediate temperatures between 150 and 200 K, the CIMS thresholds are inverted. A positive current sweep now switches the device from the P to the AP state, while a negative current sweep switches the device from the AP to the P state. The different temperature dependences of CIMS and MR suggest different origins of the physical processes involved in these two effects.

The MR effect derives from spin-dependent electron scattering in the multilayers. In 3*d* transition metals, such as Co and Fe, the number of empty states near the Fermi level is much larger in the minority than in the majority electron band. Therefore, electron scattering into these empty states is much more efficient for the minority than for the majority electrons. This spin asymmetry gives rise to the observed MR effect. In Co-rich CoGd alloys, the character of the *d* band is determined mainly by the Co subnetwork [11]. As a result, the MR effect depends primarily on the relative alignment of the moment of the Co subnetwork in the CoGd layer and that of the CoFe layer [12].

The sign reversal of MR is related to the *magnetization compensation* of the ferrimagnetic CoGd film. The Co and Gd moments in CoGd align antiparallel with each other due to ferromagnetic 4*f*-5*d* exchange coupling and 5*d*-3*d* hybridization [13,14]. The $Co_{74}Gd_{26}$ alloy used in our experiments has a magnetization compensation temperature (T_{MC}) below room temperature [10,15], at which the moments of the two subnetworks cancel each other and the alloy has no net magnetization. Above T_{MC}, the Co moment is larger than the Gd moment. Therefore, a large magnetic field aligns the Co moment parallel with the moment of the fixed layer, giving rise to a positive MR effect. Below T_{MC}, the Gd subnetwork dominates. Consequently, when a large magnetic field is applied, the Gd moment is aligned parallel with the moment of the fixed layer, while the Co moment is aligned antiparallel. As a result, the MR becomes negative.

The sign reversal of the CIMS threshold current, on the other hand, is related to the *angular momentum compensation* of the ferrimagnet. This is because CIMS is fundamentally an angular momentum transfer effect, and is thus dictated by the alignment of the net angular momentum of the CoGd layer with that of the CoFe layer. The net magnetization $\vec{M}$ and angular momentum $\vec{S}$ of CoGd can be written as follows: $\vec{M} = \vec{M}_{Co} + \vec{M}_{Gd}$ and $\vec{S} = \vec{S}_{Co} + \vec{S}_{Gd} = \vec{M}_{Co}/\gamma_{Co} + \vec{M}_{Gd}/\gamma_{Gd}$, where $\vec{M}_{Co(Gd)}$ and $\vec{S}_{Co(Gd)}$ are the magnetic moment and angular momentum of the Co(Gd) subnetwork, and $\gamma_{Co(Gd)} = g_{Co(Gd)}\mu_B/\hbar$ is the corresponding gyromagnetic ratio. Because of spin-orbit coupling on the Co site, $g_{Co} \approx 2.2$. On the other hand, $g_{Gd} \approx 2$ since the half-filled Gd 4*f* shell has no orbital angular momentum [16–18]. As a result, the angular momentum compensation temperature (T_{AMC}) is higher than T_{MC} [19]. For temperatures between T_{MC} and T_{AMC}, $\vec{M}$ and $\vec{S}$ are aligned in opposite directions. When the net magnetization of CoGd aligns parallel with that of CoFe, the net angular momentums of the two layers are actually aligned antiparallel, and vice versa. This gives rise to the sign reversal of the threshold current between 200 and 250 K.

To further understand the temperature dependence of the CIMS threshold current, we examine the Landau-Lifshiz-Gilbert equation for the net angular momentum of CoGd [1,16,20,21]:

$$\frac{d\vec{S}}{dt} = \vec{\Gamma}_H + \vec{\Gamma}_\alpha + \vec{\Gamma}_J,$$
$$= -\gamma_{\text{eff}}\vec{S} \times [\vec{H} + \vec{H}_K - 4\pi(\vec{M}\cdot\hat{z})\hat{z}] + \alpha_{\text{eff}}\gamma_{\text{eff}}\hat{s} \times \vec{S}$$
$$\times [\vec{H} + \vec{H}_K - 4\pi(\vec{M}\cdot\hat{z})\hat{z}] + a_J\hat{s} \times \hat{s}_0 \times \hat{s}, \qquad (1)$$

where $\vec{\Gamma}_H$, $\vec{\Gamma}_\alpha$, and $\vec{\Gamma}_J$ are torques exerted on CoGd by the

external field, effective damping, and spin transfer, respectively, $\alpha_{\text{eff}} = (\alpha_{\text{Co}} S_{\text{Co}} + \alpha_{\text{Gd}} S_{\text{Gd}})/|\vec{S}|$ is the effective damping coefficient, $\hat{z}$ is the unit vector of the out-of-plane axis, $\hat{s}$ and $\hat{s}_0$ are unit vectors of the angular momentum of the free and fixed layer, and $\vec{H}$, $\vec{H}_K$, and $-4\pi(\vec{M} \cdot \hat{z})\hat{z}$ are the external field, uniaxial anisotropy field, and easy-plane demagnetization field, respectively. The prefactor $a_J = (J\eta/Mt)(\hbar/2e)$ is proportional to the spin polarization (η) of the current, where J is the current density and t is the free layer thickness. The effective gyromagnetic ratio $\gamma_{\text{eff}} = M/S = (M_{\text{Co}} - M_{\text{Gd}})/(S_{\text{Co}} - S_{\text{Gd}})$ is negative inside the temperature range $T_{\text{MC}} < T < T_{\text{AMC}}$, indicating the antiparallel alignment of $\vec{M}$ and $\vec{S}$, which causes the CIMS threshold current to change sign. Physically, the reversal of the direction of $\vec{S}$ with respect to $\vec{M}$ leads to the reversal of the direction of the effective damping torque. Since the CIMS threshold current is determined by the competition between the damping torque and the spin-transfer torque, the sign of the threshold current is also reversed.

In summary, we have studied the MR and CIMS effects in spin valves with a ferrimagnetic CoGd free layer and a CoFe fixed layer at various temperatures. Different temperature dependences are observed for the MR and CIMS effects, which are attributed to distinct compensation temperatures of the net magnetization and net angular momentum of the CoGd film. Although the MR effect is often used as a means of investigating the CIMS effect, our experiments show clearly that these two phenomena have very different origins.

This work is supported by DMEA. We thank John Slonczewski for helpful discussions and Andrew Kellock for Rutherford backscattering analysis of our samples.

[1] J. C. Slonczewski, J. Magn. Magn. Mater. **159**, L1 (1996).
[2] L. Berger, Phys. Rev. B **54**, 9353 (1996).
[3] M. Tsoi *et al.*, Phys. Rev. Lett. **80**, 4281 (1998).
[4] J. A. Katine *et al.*, Phys. Rev. Lett. **84**, 3149 (2000).
[5] D. C. Ralph and R. A. Buhrman, in *Concepts in Spin Electronics*, edited by S. Maekawa (Oxford University Press, New York, 2006); J. Z. Sun, IBM J. Res. Dev. **50**, 81 (2006), and references therein.
[6] P. Chaudhari, J. J. Cuomo, and R. J. Gambino, Appl. Phys. Lett. **22**, 337 (1973); P. Hansen, C. Clausen, G. Much, M. Rosenkranz, and K. Witter, J. Appl. Phys. **66**, 756 (1989).
[7] J. Z. Sun *et al.*, J. Appl. Phys. **93**, 6859 (2003).
[8] S. I. Kiselev *et al.*, Nature (London) **425**, 380 (2003).
[9] R. C. Taylor and A. Gangulee, J. Appl. Phys. **47**, 4666 (1976); **48**, 358 (1977).
[10] C. Kaiser, Ph.D. thesis, RWTH Aachen, Germany, 2005, and references therein.
[11] S. K. Malik, F. J. Arlinghaus, and W. E. Wallace, Phys. Rev. B **16**, 1242 (1977); H. Tanaka and S. Takayama, J. Appl. Phys. **70**, 6577 (1991).
[12] C. Bellouard *et al.*, Phys. Rev. B **53**, 5082 (1996).
[13] I. A. Campbell, J. Phys. F **2**, L47 (1972).
[14] S. S. Anilturk and A. R. Koymen, Phys. Rev. B **68**, 024430 (2003).
[15] C. Kaiser, A. F. Panchula, and S. S. P. Parkin, Phys. Rev. Lett. **95**, 047202 (2005).
[16] C. Kittel, Phys. Rev. **76**, 743 (1949).
[17] G. G. Scott, Rev. Mod. Phys. **34**, 102 (1962).
[18] B. I. Min and Y.-R. Jang, J. Phys. Condens. Matter **3**, 5131 (1991).
[19] C. D. Stanciu *et al.*, Phys. Rev. B **73**, 220402(R) (2006).
[20] R. K. Wangsness, Phys. Rev. **91**, 1085 (1953).
[21] We assume that the exchange interaction between the Co and Gd subnetworks is strong enough to ensure a rigid antiparallel alignment of their magnetization and angular momentum.